



ELSEVIER

Marine Micropaleontology 36 (1999) 13–30

MARINE  
MICROPALAEONTOLOGY

## Calcareous nannofossil biostratigraphy of the M. del Casino section (northern Apennines, Italy) and paleoceanographic conditions at times of Late Miocene sapropel formation

A. Negri<sup>a,\*</sup>, S. Giunta<sup>b</sup>, F. Hilgen<sup>c</sup>, W. Krijgsman<sup>d</sup>, G.B. Vai<sup>b</sup>

<sup>a</sup> Istituto di Scienze del Mare, University of Ancona, Via Brezze Bianche, 60131 Ancona, Italy

<sup>b</sup> Dipartimento di Scienze della Terra e Geologico Ambientali, University of Bologna, Via Zamboni 67, 40100 Bologna, Italy

<sup>c</sup> Department of Geology, Institute of Earth Sciences, Budapestlaan 4, 3584 CD Utrecht, The Netherlands

<sup>d</sup> Paleomagnetic Laboratory, Fort Hoofddijk, Budapestlaan 17, 3584 CD Utrecht, The Netherlands

Received 9 March 1998; accepted 11 August 1998

### Abstract

A detailed quantitative calcareous nannofossil analysis has been performed on 138 samples from the astronomically dated Monte del Casino section with the aim to identify and precisely date the most important calcareous nannofossil events across the Tortonian/Messinian boundary in the Mediterranean, and to unravel paleoceanographic conditions at times of sapropel formation during the Late Miocene. From the biostratigraphic perspective, the genus *Amaurolithus* provides three successive first occurrences (FOs): *A. primus*, *A. cf. amplificus* and *A. delicatus*, dated at 7.446, 7.434 and 7.226 Ma, respectively. Other bioevents include the base and top of the 'small reticulofenestrads' Acme, dated at 7.644 and 6.697 Ma, and the FO, FCO and LO of *R. rotaria*, dated at 7.405, 7.226 and 6.771 Ma. These events appear to be useful in improving biostratigraphic resolution in the Tortonian–Messinian boundary interval, at least for the Mediterranean. Quantitative analysis revealed changes in the calcareous nannofossil assemblage associated with the sapropels. The observed fluctuations suggest a single mechanism for sapropel formation in the Mediterranean during the late Neogene. Sapropels are characterized by a decrease in the total number of coccoliths, interpreted mainly as a reduction in calcareous nannofossil production due to increased siliceous plankton production during spring blooms; and an increase in reworked specimens, interpreted to reflect enhanced continental input via river run-off. An increase in abundance of the genus *Rhabdosphaera* can be explained by opportunistic behavior at the end of the spring bloom when nutrient levels start to become impoverished. As far as sea surface water temperature indicators are concerned, warm water *D. pentaradiatus* shows positive fluctuations in sapropels while cooler water *D. intercalaris* and *C. pelagicus* show negative fluctuations. © 1999 Elsevier Science B.V. All rights reserved.

**Keywords:** Mediterranean area; Late Miocene; biostratigraphy; calcareous nannofossils; sapropel

\* Corresponding author. Fax: +39-71-220-4650; E-mail: anegri@popcsi.unian.it

## 1. Introduction

During the last 5 years, progress has been made in dating marine successions of late Tortonian to early Messinian age in the Mediterranean, resulting in a much older age for the T/M boundary than previously thought. The new age control with its unprecedented accuracy and resolution is of special importance if one strives to understand the complexity of processes that ultimately led to the (onset of the) Messinian salinity crisis. In 1993, radiometric dating of biotites obtained from volcanic ash layers in the Monte del Casino and Monte Tondo sections (northern Apennines) led to an age of 7.26 Ma for the T/M boundary (Vai et al., 1993). A re-evaluation of magnetostratigraphy including new data and cyclostratigraphic information from sections on Crete resulted in an age of 6.92 Ma for the T/M boundary according to the geomagnetic polarity time scale of Cande and Kent (1995) (Krijgsman et al., 1994). The radiometric age of Vai et al. (1993) has subsequently been confirmed and refined — to 7.240 Ma — by the astronomical dating method which relies on tuning sedimentary cycle patterns to astronomical time series which describe the past variations in the Earth's orbital parameters (Krijgsman et al., 1995; Hilgen et al., 1995).

The latter studies resulted in an integrated stratigraphic framework, which is astronomically dated and includes cyclostratigraphy, magnetostratigraphy, and planktonic foraminiferal and dinoflagellate cyst biostratigraphy via first order calibration. Thus far a detailed calcareous nannofossil biostratigraphy is lacking. A previous study (Negri and Vigliotti, 1997) revealed difficulties in applying the standard zonations of Martini (1971) and Okada and Bukry (1980). The only useful event is the FO of the horseshoe shaped genus *Amaurolithus*. This event proved to approximate the T/M boundary and despite its scarcity has been adopted in the Mediterranean as well (Colalongo et al., 1979).

In this paper, we present the results of a detailed calcareous nannofossil study of the Monte del Casino section with the aim of improving the resolution of the Upper Miocene biostratigraphy within the framework of the integrated and astronomically dated stratigraphy (Krijgsman et al., 1997). The second aim of the paper is an attempt to understand

cyclic fluctuations in the calcareous nannofossil assemblages in terms of paleoceanographic changes leading to the deposition of sapropels.

## 2. Materials and methods

The Monte del Casino section located in the foothills of the northern Apennines (Fig. 1) contains a well-exposed, open marine succession of upper Tortonian–lower Messinian marly clays with numerous biotite-rich ash layers and cyclic intercalations of brown to black, organic carbon-rich, laminated sediments, termed sapropels. Initial problems encountered in sampling and logging a continuous undisturbed succession (Vai et al., 1993) were solved after careful logging of overlapping sections in different gullies (Krijgsman et al., 1997). In this way, it was possible to eliminate almost completely the disturbing effect of low-angle shearplanes. The section which straddles the T/M boundary has been subject of a number of studies to which the reader is referred for more detailed information about the geologic setting (Calieri, 1992; Vai et al., 1993; Ferretti and Terzi, 1995; Negri and Vigliotti, 1997; Calieri, 1997; Krijgsman et al., 1997). The samples and lithological log of the present study are the same as in Krijgsman et al. (1997). Hundred thirty-eight samples with an average spacing of 20 cm (Fig. 2) were used for a detailed calcareous nannofossil analysis. Sample preparation followed standard techniques. A settled slide was mounted with Norland Optical Adhesive. No centrifugation was applied to concentrate the biogenic fraction in order to retain the original composition of the nannofossil assemblage. The settling technique — processing a constant volume of sediment — was adopted following the methodology reported in De Kaenel and Villa (1996). This technique provides the advantage of a uniform dispersion of coccoliths over the slide. Quantitative analyses were performed following the methodology described in Rio et al. (1990), with a light microscope at  $\times 1250$  magnification and counting at least 300 specimens per sample. The area in which the analysis was performed (i.e. number of fields of view) was used to convert the frequencies of the species counted to number/mm<sup>2</sup>. Additional counts of up to at least 100 specimens were done for the

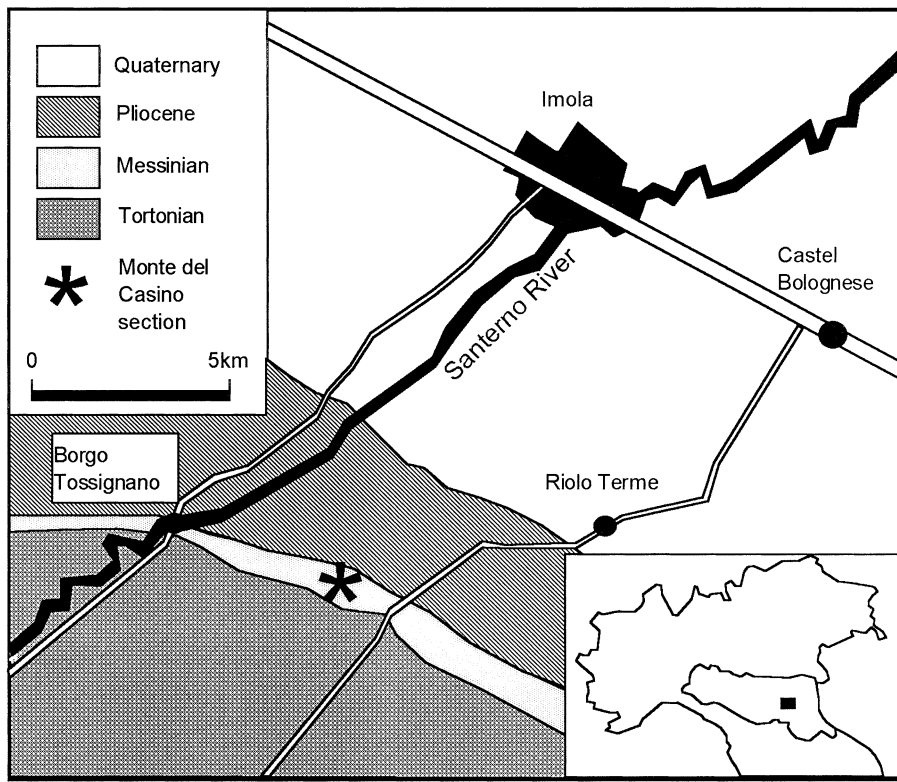


Fig. 1. Location map of the Monte del Casino section in the northern Apennines (Italy).

genera *Helicosphaera* and *Discoaster*. The values obtained were converted to percentages to obtain the frequency of each species within the genus.

As for the very rare *Amaurolithus* group, frequencies were estimated by counting the number of specimens encountered in 1000 fields of view at  $\times 1250$  magnification ( $22.22 \text{ mm}^2$ ). Finally, the number of 'small reticulofenestrids' (with the long axis  $< 3 \mu\text{m}$ ) was counted in a single field of view to estimate the frequency of this taxon. In both cases results were later converted to number/ $\text{mm}^2$ . The reproducibility of all absolute value of specimens (in number/ $\text{mm}^2$ ) is assured by the high precision methodology adopted for the preparation of the sample (De Kaenel and Villa, 1996).

### 3. Results

Calcareous nannofossils are abundant and generally well preserved in all samples. Nannofossil as-

semblages consist mainly of *Coccolithus pelagicus*, *Calcidiscus leptoporus*, *Geminolithella rotula*, *Rhabdosphaera claviger*, *Rhabdosphaera styliifer*, *Syracosphaera pulchra*, *Syracosphaera* spp. and *Reticulofenestra* spp., whereas *Scyphosphaera* spp., *Pontosphaera* spp., *Braarudosphaera* spp. and *Thorasphaera* spp. are rare and discontinuous throughout the section. The assemblage is dominated by the 'small reticulofenestrids' (*Reticulofenestra minuta* and *Dictyococcites productus*) in the interval between 1.47 and 30.47 m (Fig. 3). The first occurrence (FO) of *Reticulofenestra rotaria* is found at 9.81 m whereas the first common occurrence (FCO) of this species is recorded at 16.06 m. The frequency curves of the genus *Amaurolithus* reveal the successive FO's of *Amaurolithus primus* at 8.37 m, of *Amaurolithus* cf. *amplificus* at 8.85 m and of *Amaurolithus delicatus* at 16.06 m, the latter coincident with the FO of *R. rotaria*. The occurrence of some *Triquetrorhabdulus/Amaurolithus* intergrade forms (Plate 1) between 25.30 and 29.33 m is remark-

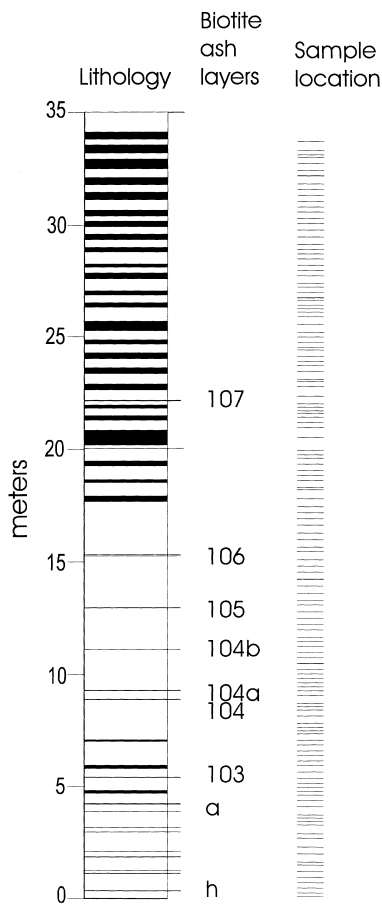


Fig. 2. Monte del Casino section columnar log. Black = sapropel; white = hemipelagic marls.

able. The genus *Helicosphaera* is well represented and dominated by *Helicosphaera carteri*, and subordinate *Helicosphaera intermedia* (Fig. 4). *Helicosphaera orientalis* and *Helicosphaera stalis* are discontinuously present but a negative overall trend in abundance can be observed towards the top of the section. *Helicosphaera walbersdorfensis* is also rare and discontinuous but this species shows an opposite trend with respect to *H. orientalis* and *H. stalis* marked by a slight increase in abundance towards the top of the section. *Helicosphaera sellii* is rare and discontinuously present from the base of the studied interval but becomes more abundant in the upper part the section.

The genus *Discoaster* is generally abundant (Fig. 5), but preservation varies from poor to good;

the best preserved specimens are encountered in sapropel samples. Most of the specimens belong to *Discoaster variabilis* and *Discoaster pentaradiatus*. *Discoaster brouweri* and *Discoaster intercalaris* are commonly recorded, while *Discoaster challengeri* and *Discoaster icarus* are rare. Very rare specimens of *Discoaster loeblichii* were found in the lower part of the section. Finally, *Discoaster tamalis* and *Discoaster asymmetricus* are remarkable albeit rare constituents of the assemblage as already noticed by Krijgsman et al. (1997). The frequency curve of *Rhabdosphaera* spp. is shown in Fig. 5. Strong fluctuations in the abundance of *Rhabdosphaera* spp. are observed with peak values being reached in the sapropels. As far as the discoasterids are concerned, *D. pentaradiatus* is marked by positive fluctuations related to the sapropels whereas *D. intercalaris* shows negative fluctuations in the sapropels. The placolith *C. pelagicus* shows also a decrease in abundance in sapropels (Fig. 5).

The preservation of calcareous nannofossils appear to improve in sapropels. The number of reworked specimens (whose ages range from the Late Cretaceous to the Middle Miocene) reaches maximum values in sapropels, while the total number of (calcareous nannofossil) specimens reach minimum values (Fig. 5). An increase in the abundance of calcareous spicules (probably belonging to planktic foraminifers) and diffuse pyrite is observed in all sapropel samples. Finally, amorphous organic matter, brown to dark brown colored under the light microscope, is commonly found and abundant in the sapropels.

#### 4. Biostratigraphy

Our biostratigraphic analysis yielded a number of calcareous nannofossil events (Table 1; Fig. 6) that appear to be useful to improve the biostratigraphic resolution of the time interval straddling the T/M boundary.

##### 4.1. Acme Begin (AB) and Acme Top (AT) of 'small' reticulofenestrads

A Late Miocene increase in 'small placoliths', i.e. reticulofenestrads having the long axis smaller

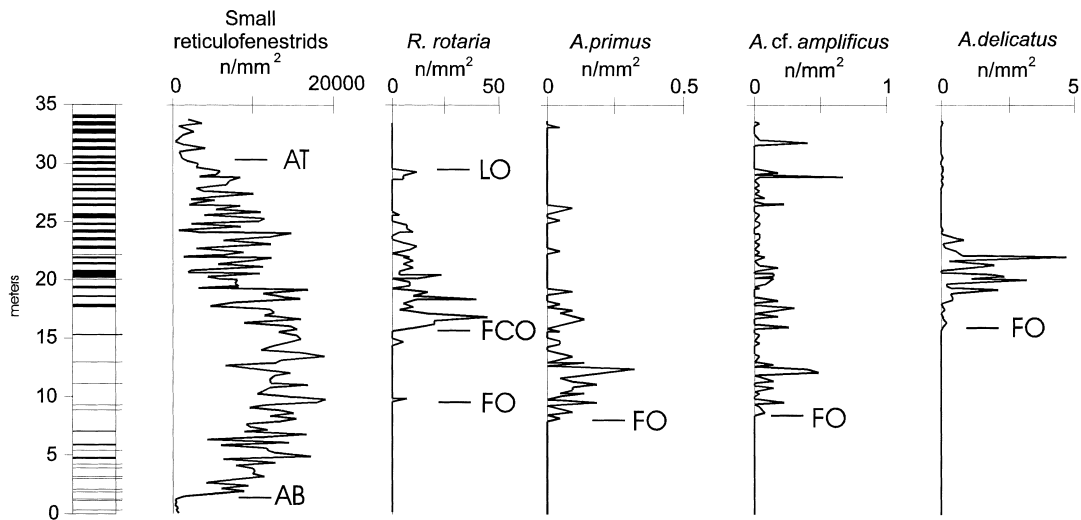


Fig. 3. Frequency curve of the most important biostratigraphic markers ('small' reticulofenestrads, *R. rotaria*, *A. primus*, *A. cf. amplificus*, *A. delicatus*). AB = Acme Begin; AT = Acme Top; FCO = first common occurrence; FO = first occurrence; LO = last occurrence.

than 3  $\mu\text{m}$ , has been observed by several authors (Backman, 1978; Flores and Sierró, 1987; Gartner, 1992; Sierró et al., 1993). This increase is observed within subzone CN9a between the *D. berggrenii* and *A. primus* FO's. Although this increase is likely related to some ecological factor, Flores et al. (1992) demonstrated that this event is synchronous between the Spanish and Moroccan corridors and Northeast Atlantic DSDP sites. In Mediterranean ODP Site 654, the increase in small reticulofenestrads was not detected even though a clear dominance of small placoliths can be observed in fig. 3 of Flores et al. (1992). The base of the small reticulofenestrads Acme is probably located below core 45 where they started their analysis.

In the Monte del Casino section, the increase in small reticulofenestrads is found between 1.49 and 1.79 m, and corresponds to Chron C4n. The astronomically interpolated age is 7.644–7.532 Ma. This position is in good agreement with the existing literature. In the top part of the section, a decrease in the abundance of the small reticulofenestrads is observed between 30.47 and 30.83 m and the interpolated age is 6.697–6.687 Ma. This event — tentatively defined as Acme Top (AT) — has not been reported before. Further studies are needed to confirm the usefulness and reliability of this event.

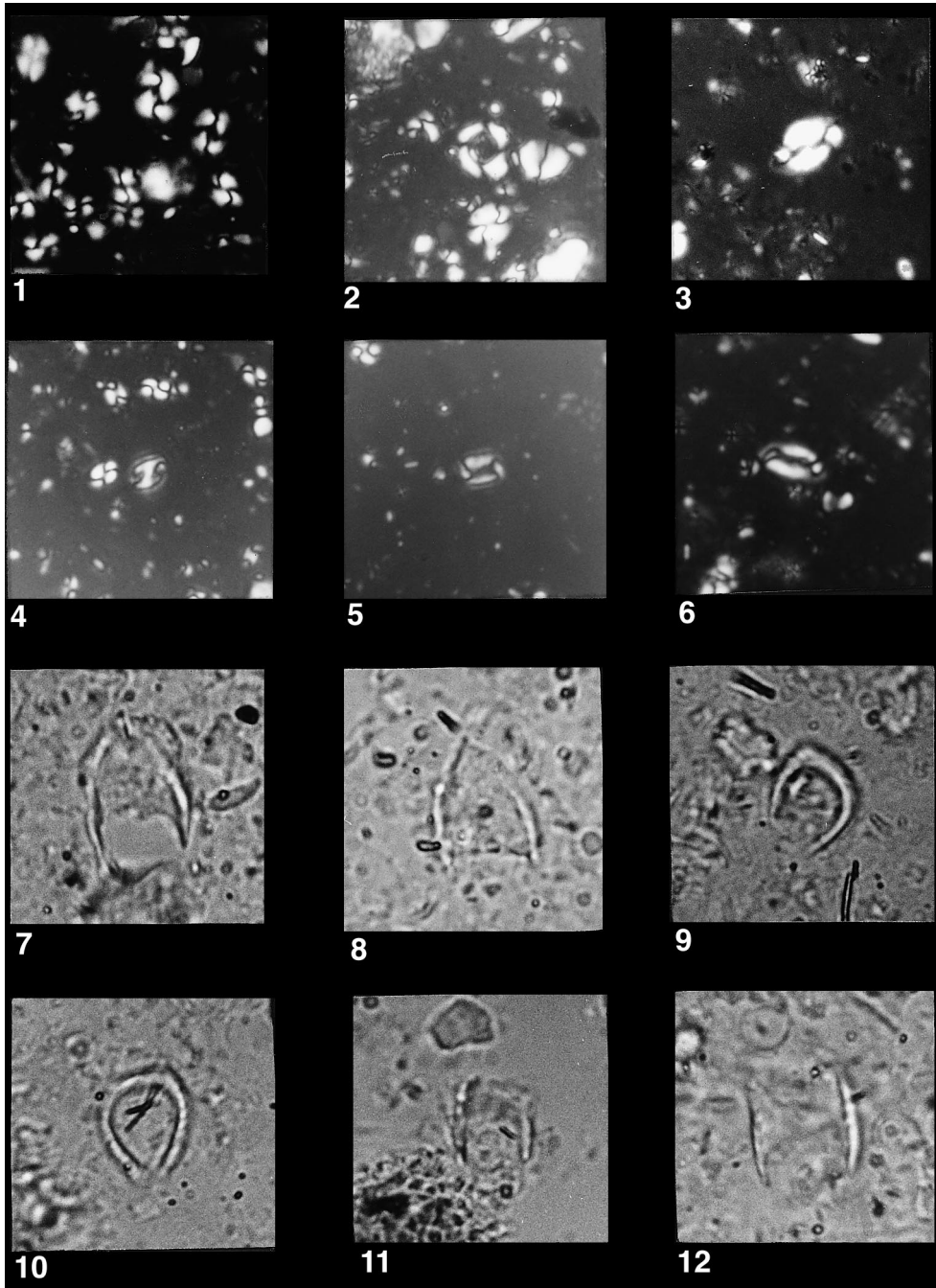
#### 4.2. *Amaurolithus primus* FO

The FO of the horseshoe shaped *Amaurolithus*, which defines the CN9a/CN9b subzonal boundary in the biostratigraphic scheme proposed by Okada and Bukry (1980), is currently adopted by calcareous nannofossil specialists to approximate the T/M boundary in the open ocean. This event, however, clearly predates the FO of *Globorotalia conomiozea*, the planktic foraminiferal event used to define the boundary in the Mediterranean. Due to their scarcity, several specialists do not differentiate between *Amaurolithus* species and label them together as *Amaurolithus* spp. For instance, Negri and Vigliotti (1997) and Krijgsman et al. (1997) recognize only the FO of *Amaurolithus* spp. in previous studies of the Monte del Casino section while Gartner (1992) recorded the *Amaurolithus* spp. FO event (likely *A. primus* FO) in a magnetostratigraphically not well defined interval above Chron C4 in the North Atlantic (Fig. 6).

Other researchers, however, distinguish events at the species level. In the Sale Briqueterie drill core (northwestern Morocco), Hodell et al. (1994) found the FO of *A. primus* in Chron C4n.2n whereas Rakic El Bied and Benson (1996) recorded the same event at a slightly younger level, at the C3Bn/C3Br boundary, in the Ain el Beida section located nearby. In the

equatorial Pacific and Indian Ocean, the FO of *A. primus* is recorded in Chron C3Br (Raffi et al., 1995), while, in the Mediterranean, this event is detected

in former Chron 6, equivalent to the C3Bn/C3Br boundary (Flores et al., 1992) (Fig. 6). As shown in Fig. 6, the subchronozonal designation of the



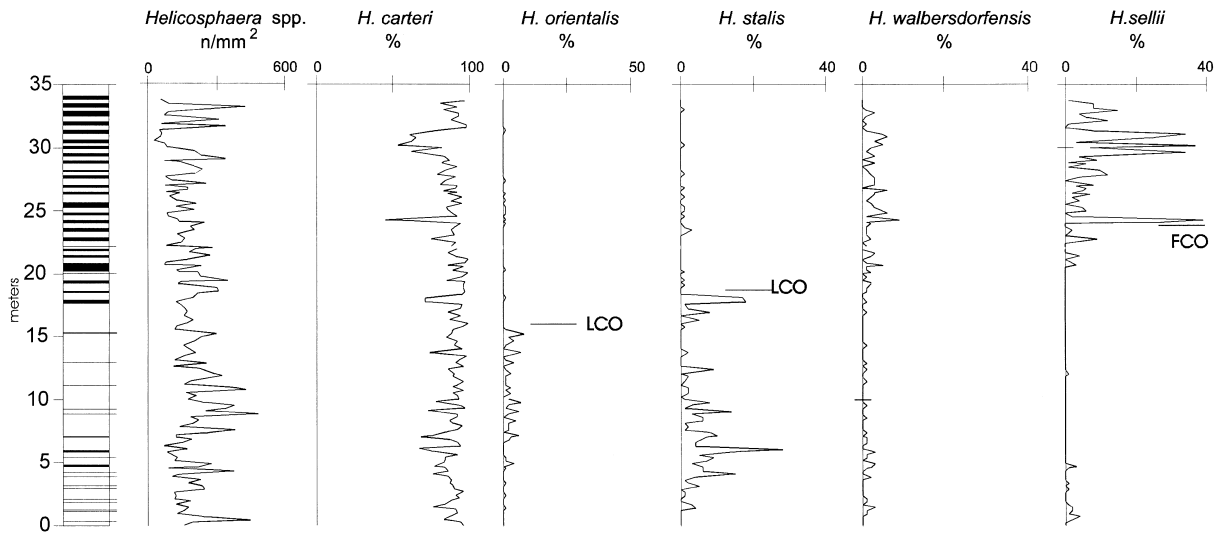


Fig. 4. Frequency curves of Helicoliths. *Helicosphaera* spp. are expressed in number/mm<sup>2</sup>. Percentages of *H. carteri*, *H. orientalis*, *H. stalis*, *H. walbersdorfensis*, and *H. sellii* calculated on 100 Helicoliths. LCO = last common occurrence; FCO = first common occurrence.

FO of *A. primus* differs slightly in the literature. This is probably due to the scarcity of *Amaurolithus* in the sediment and to the different analysis method. However, despite the discrepancies, the *A. primus* FO is an important event which may be demonstrated to be more synchronous if the same quantitative techniques are applied (e.g., Raffi et al., 1995; this study). The detailed magnetostratigraphy of the Monte del Casino section allows us to locate the *A. primus* FO in Chron C3Br.2r, giving an age between 7.455 and 7.301 Ma for this event. Interpolation of the sedimentation rate using the astronomically dated sapropels C17 and C18 as calibration points yields a more precise age estimate of 7.446–7.440 Ma.

#### 4.3. *Amaurolithus cf. amplificus* FO

*A. amplificus* is a very large species (12–20  $\mu\text{m}$ ), the FO of which is found in Chron C3An in the open ocean (Raffi and Flores, 1995; Raffi et al., 1995), i.e. well above the *G. conomiozea* FO. Several authors, however, observed the first occurrence of this species at lower levels. For instance, Colalongo et al. (1979) placed the *A. amplificus* FO slightly above the FO of *A. primus* in their integrated biostratigraphic scheme. The same closely spaced sequence of events has also been recognized in the Guadalquivir basin (Flores and Sierro, 1987) and in the Tortonian type section of Rio Mazzapiedi–Castellania (Mazzei et al., 1979). In the Monte del Casino section, we found

#### Plate 1

1. 'Small' reticulofenestrids assemblage, sample CAS 192, crossed nicols.  $\times 1875$ .
2. *Reticulofenestra. rotaria* Theodoridis, 1984, sample CAS 28, crossed nicols.  $\times 2000$ .
3. *Helicosphaera sellii* Bukry and Bramlette, 1969, sample CAS 80, crossed nicols.  $\times 1785.7$ .
4. *Helicosphaera stalis* Theodoridis, 1984, sample CAS 204, crossed nicols.  $\times 1875$ .
5. *Helicosphaera orientalis* Black, 1971, sample CAS 204, crossed nicols.  $\times 1875$ .
6. *Helicosphaera walbersdorfensis* (Müller) Theodoridis, 1984, sample CAS 86, crossed nicols.  $\times 1667$ .
7. *Amaurolithus primus* (Bukry and Percival) Gartner and Percival, 1975, sample CAS 88, parallel nicols.  $\times 2083$ .
8. *Amaurolithus primus* (Bukry and Percival) Gartner and Percival, 1975, sample CAS 88, parallel nicols.  $\times 2083$ .
9. *Amaurolithus delicatus* Gartner and Bukry, 1975, sample CAS 64, parallel nicols.  $\times 1875$ .
10. *Amaurolithus delicatus* Gartner and Bukry, 1975, sample CAS 64, parallel nicols.  $\times 1875$ .
11. Intergrade form (?), *Triquetrorhabdulus–Amaurolithus*, sample CAS 88, parallel nicols.  $\times 1500$ .
12. Intergrade form (?), *Triquetrorhabdulus–Amaurolithus*, sample CAS 88, parallel nicols.  $\times 2344$ .

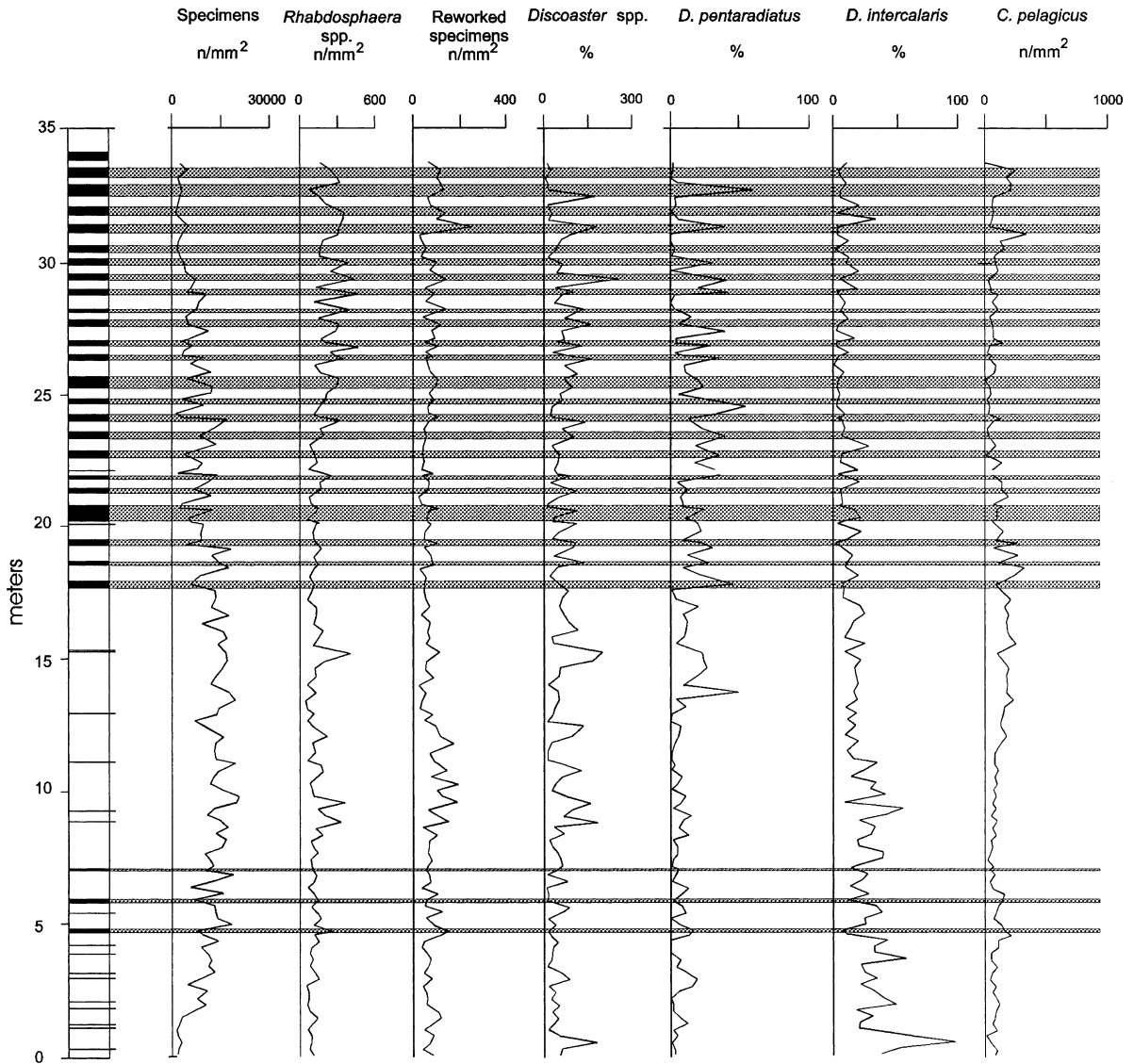


Fig. 5. Frequency curves of the taxa showing consistent relationships to sapropels: Frequencies of the total number of specimens, *Rhabdosphaera* spp. *Discoaster* spp. *C. pelagicus* and reworked specimens are expressed in number/mm<sup>2</sup>. Percentages of *D. pentaradiatus* and *D. intercalaris* are calculated on 100 discoasters.

specimens similar to *A. amplificus* but with smaller dimensions (8  $\mu\text{m}$ ) starting from a level 50 cm above the *A. primus* FO. These specimens cannot be confused with *A. primus* but also cannot be attributed to *A. amplificus* because of their smaller dimensions. In this paper we provisionally label these specimens as *A. cf. amplificus*; however, a clear definition of the *A. amplificus* species concept is needed. In this way, our *A. cf. amplificus* FO is likely to correspond to

the *A. amplificus* FO in Colalongo et al. (1979) and Flores and Sierro (1987). According to the magnetostratigraphy of Krijgsman et al. (1997) the event is recorded in Chron C3Br.2r with an attributed age between 7.455 and 7.301 Ma. The more precise astronomical age calculated by means of interpolation of the sediment accumulation rate is 7.434–7.428 Ma. The event is almost coincident with the *A. primus* FO.

Table 1  
Biostratigraphic events in the Monte del Casino section and their astronomically derived ages

Biostratigraphic events		Level (m)	Chron	Astronomically derived age (Ma)
AT	'small' reticulofenestrads	30.47–30.83	C3Ar	6.697–6.687
LO	<i>R. rotaria</i>	29.33–29.65	C3Ar	6.771–6.760
FCO	<i>H. sellii</i>	24.01–24.13	C3Ar	6.968–6.964
LCO	<i>H. stalis</i>	18.10–18.40	?	7.159–7.151
FCO	<i>R. rotaria</i>	15.81–16.06	?	7.226–7.218
FO	<i>A. delicatus</i>	15.81–16.06	?	7.226–7.218
LCO	<i>H. orientalis</i>	15.56–15.81	?	7.233–7.226
FO	<i>R. rotaria</i>	9.57–9.81	C3Br.2r	7.405–7.398
FO	<i>A. cf. amplificus</i>	8.61–8.85	C3Br.2r	7.434–7.428
FO	<i>A. primus</i>	8.13–8.37	C3Br.2r	7.446–7.440
AB	'small' reticulofenestrads	1.49–1.73	C4n.1n	7.644–7.532

4.4. Reticulofenestra rotaria FO and FCO

The FO of *R. rotaria* was first used by Theodoridis (1984) to define the base of the *R. rotaria* zone in his biostratigraphic scheme for the Mediter-

anean Miocene. We distinguish between FO and FCO since the two events are clearly separated. In his work, Theodoridis (1984) only performed a qualitative biostratigraphic analysis and, most likely, he did not detect the true FO of this rare species but

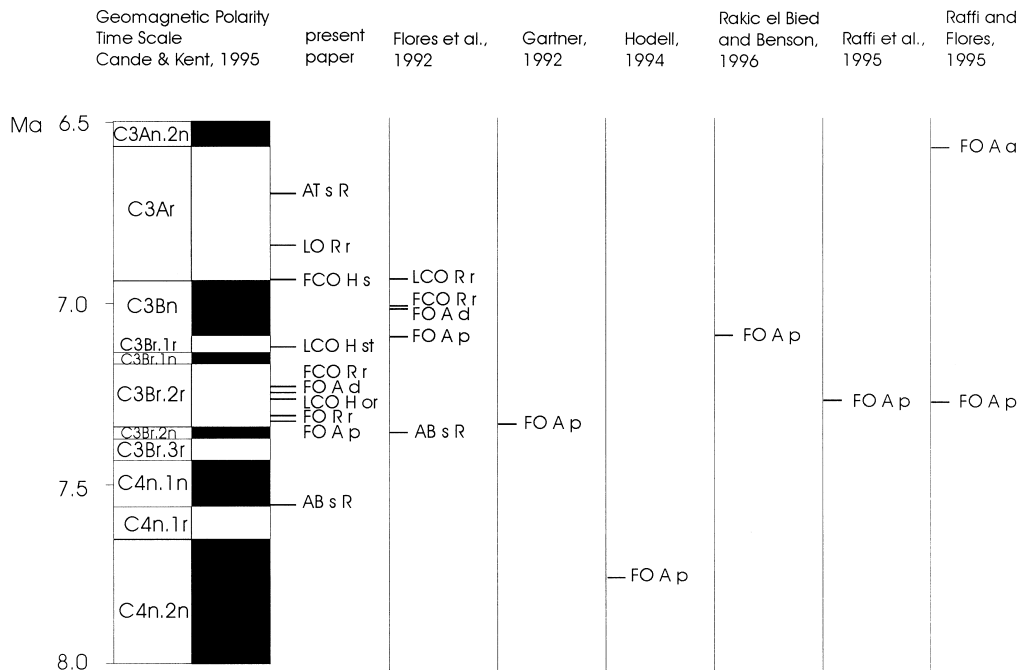


Fig. 6. Comparison of the stratigraphic position of the proposed events in the present paper versus the ones recorded by different authors. *AB s R* = Acme Begin 'small' reticulofenestrads; *FO A p* = first occurrence *A. primus*; *FO R r* = first occurrence *R. rotaria*; *LCO H or* = last common occurrence *H. orientalis*; *FO A d* = first occurrence *A. delicatus*; *FCO R r* = first common occurrence *R. rotaria*; *LCO H st* = last common occurrence *H. stalis*; *FCO H s* = first common occurrence *H. sellii*; *LO R r* = last common occurrence *R. rotaria*; *AT s R* = Acme Top 'small' reticulofenestrads.

only the FCO. As a consequence, the base of his *R. rotaria* zone is likely defined by the *R. rotaria* FCO.

The FO of *R. rotaria* in our study is observed very close to the *A. primus* FO. The FO is followed by a prolonged interval in which the species is absent. The FCO is located much higher in the section — at 16.06 m — and coincides with the *A. delicatus* FO.

The *R. rotaria* FCO has been detected invariably above the *A. primus* FO, both in Mediterranean (Fig. 6; Guercif Basin — Tazzi, 1996; ODP Site 654 — Flores et al., 1992) as well as in extra-Mediterranean successions such as ODP sites 846, 849 and 850 in the equatorial Pacific (Raffi and Flores, 1995). In the Mediterranean, the FCO is recorded slightly above the *A. delicatus* FO at ODP Site 654 (Flores et al., 1992) and in the Falconara section (Theodoridis, 1984). It is thus likely that all specialists have been observing the *R. rotaria* FCO (and not the FO). The *R. rotaria* FCO is easily correlatable between the different sections. In particular, the excellent agreement with ODP Site 654 in the Tyrrhenian Sea indicates that this event is synchronous on at least a Mediterranean scale. The FO of *R. rotaria* is recorded in Chron C3Br.2r and has an astronomical age of 7.405–7.398 Ma. Unfortunately, the lack of a consistent magnetostratigraphic signal hampers a direct first-order correlation of the *R. rotaria* FCO to a specific chron. But on the basis of detailed cyclostratigraphic correlations of other Mediterranean sections (Krijgsman et al., 1997, fig. 10) the correlation of *R. rotaria* FCO to Chron C3Br.1r is possible. Its astronomical age falls between 7.226 and 7.218 Ma.

#### 4.5. *Helicosphaera orientalis* LO

The LO of *H. orientalis* is located above the *R. rotaria* LO according to Theodoridis (1984). In his range chart, the occurrence of *H. orientalis* is marked by hatchure pattern from the *R. rotaria* FO to its extinction level, probably indicating discontinuity and also rarity. However, his qualitative approach makes it difficult to ascertain whether he recorded both the LCO and LO of the species. Negri and Vigliotti (1997), lumping *H. orientalis* together with *H. stalis* and *H. walbersdorfensis*, observed a marked drop in abundance between the base of the section and the LCO of the lump category close to the *A. delicatus* FO. In our record, the LCO of *H. orientalis* (within

the genus *Helicosphaera*) is recorded directly below the *A. delicatus* FO and *R. rotaria* FCO. This position is not in agreement with the LO of Theodoridis (1984), indicating that his event is not consistent with our LCO. In our study the astronomical age for the LCO is dated at 7.233–7.226 Ma. But the opposite abundance fluctuations of *H. stalis* and *H. orientalis* suggest that their presence is controlled by local paleoecological factors and, hence, that they may not be useful for time stratigraphic correlations.

#### 4.6. *Amaurolithus delicatus* FO

This event was previously recognized by Colalongo et al. (1979) to be close to the *G. conomiozea* FO and thus appears to represent the best biostratigraphic approximation of the Tortonian/Messinian boundary by means of calcareous nannofossils. Theodoridis (1984) found the *A. delicatus* FO to be positioned slightly above the *A. primus* FO and slightly below the *R. rotaria* FCO. The same succession of events is also reported by Flores et al. (1992) from ODP Site 654 where the *A. delicatus* FO is observed in the middle part of former Chron 6 (Fig. 6). Raffi and Flores (1995) detected the same event directly above the *A. primus* FO in Chron C3Br.1r (Fig. 6). At Monte del Casino, the *A. delicatus* FO is found slightly below Chron C3Bn in an interval that is characterized by a very poor magnetostratigraphic signal. Detailed cyclostratigraphic correlations to other Mediterranean sections indicate that the event correlates with Chron C3Br.1r (Krijgsman et al., 1997, fig. 10). The astronomical age for the event is 7.226–7.218 Ma.

#### 4.7. *Helicosphaera stalis* LCO

Our results for the LCO of *H. stalis* are very similar to that of *H. orientalis*. According to Theodoridis (1984), the LO of *H. stalis* is recorded above the *R. rotaria* LO but in his range chart the distribution of *H. stalis* is indicated by a hatchure pattern between the *R. rotaria* LO and its own extinction, probably indicating discontinuity and also rarity. As with *H. orientalis* it is difficult to establish whether or not he recognizes both the LCO and LO. As mentioned above, Negri and Vigliotti (1997) lumped this species together with *H. orientalis* and *H. walbersdorfensis*,

reporting the LCO of the lump category close to the *A. delicatus* FO. In our record, we observe a *H. stalis* LCO followed by a discontinuous range which starts from the level of the *A. delicatus* FO and *R. rotaria* FCO. The position of the event appears to be in contrast with both Theodoridis (1984) and Negri and Vigliotti (1997). For this reason, we are of the opinion that *H. stalis* is not very useful for stratigraphic purposes. The astronomical age of the LCO is 7.159–7.151 Ma.

#### 4.8. Reticulofenestra rotaria LO

The LO of *R. rotaria* is observed in the top part of the section, corresponding to a position within Chron C3Ar. Theodoridis (1984), in his biostratigraphic scheme, used this event to define the top of the *R. rotaria* zone. In the Falconara section studied by Theodoridis, the event is located 10 m below the evaporites of the Gessoso–Solfifera Formation, i.e. in overall agreement with our data. In ODP Site 654, Flores et al. (1992) report this event from the top of Chron 6n which, following the codification of Cande and Kent (1992), corresponds to C3Bn. In our record, the *R. rotaria* LO is observed at a slightly younger position within the top part of C3Ar. The astronomically derived age for this event is 6.771–6.760 Ma.

#### 4.9. Helicosphaera sellii FCO

*H. sellii* is present from the base of the section but its distribution becomes more continuous only from a level much higher in the section where we place the *H. sellii* FCO. Flores and Sierro (1987) previously reported the presence of rare specimens named *H. cf. sellii* in sections of the Guadalquivir basin and De Kaenel and Villa (1996) reported *H. sellii* in the Late Miocene of the ODP Leg 149 Hole 900a from the Iberia Abyssal Plain. Finally, Negri and Vigliotti (1997) also noticed the presence of *H. sellii* in a previous study of the Monte Tondo and Monte del Casino sections. In our record we detect the *H. sellii* FCO at the base of Chron C3Ar with an astronomical age of 6.968–6.964 Ma. The FO of this species is currently adopted to define the MNN 12/MNN 13 boundary in the Mediterranean zonal scheme of Rio et al. (1990); we postulate that the Pliocene appearance marks a re-entry of this

species after the ending of the Messinian salinity crisis in the Mediterranean. If the *H. sellii* FCO observed at Monte del Casino is confirmed in other Mediterranean sections, a redefinition of the Pliocene event as Paracme End will be necessary.

#### 4.10. Biostratigraphic resolution

We report 11 potentially useful events (Table 1; Fig. 7) in a time interval of 1 Ma. If these are confirmed from other Mediterranean sections they will provide an improvement in the biostratigraphic resolution of a key interval as the Tortonian/Messinian boundary. Further the integration of the calcareous nannofossil data with the planktic foraminifers biostratigraphy will provide a high stratigraphic resolution for the definition of the Tortonian–Messinian Boundary Global Stratotype Section and Point (GSSP) and will represent an essential framework for further chronological refinements.

### 5. Paleoclimatic and paleoceanographic considerations

Similarly to the late Quaternary Mediterranean sapropels, Miocene sapropels represent a scientific problem. They also consist of dark colored organic carbon-rich layers interbedded in the normal pelagic (or hemipelagic) sediments of the Mediterranean sea. The deposition of Quaternary sapropels appears to be related to significant changes in climate, circulation and biogeochemical cycling. Over the past 30 years many papers have been published dealing with this topic, and a series of hypotheses about the origin of sapropels have been proposed.

The origin of Quaternary sapropels was originally related to two mutually exclusive causes: (1) anoxia in the bottom water causing organic matter preservation (Olausson, 1961; Ryan, 1972; Thunell et al., 1977; Cita et al., 1977; Thunell, 1979; Rossignol Strick, 1983, 1985); (2) enhanced primary productivity in the photic zone (Calvert, 1983; Parisi, 1987; Pedersen and Calvert, 1990; Violanti et al., 1991). Since neither of the above causes was sufficient to explain such layers, Rohling and Gieskes (1989) proposed a model of deposition for Quaternary sapropels S-3, S-4 and S-5 that combined the two causes.

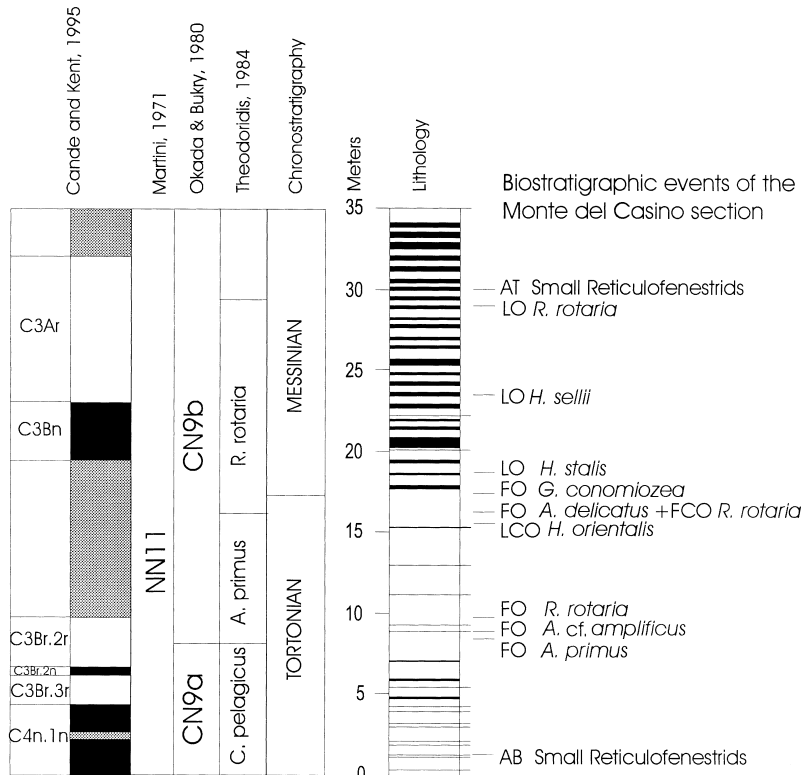


Fig. 7. Biostratigraphic events in the Monte del Casino section in the framework of the Geomagnetic Polarity Time Scale (Cande and Kent, 1995), of the standard calcareous nannofossil biostratigraphic zonations (Martini, 1971; Okada and Bukry, 1980) and of the Mediterranean zonation of Theodoridis (1984). *G. conomiozea* FO after Calieri, 1997. AB = Acme beginning; AT = Acme top; FCO = first common occurrence; FO = first occurrence; LO = last occurrence; LCO = last common occurrence.

According to this model, the formation of sapropels resulted from an increased new production in a Deep Chlorophyll Maximum (DCM) coupled with a reduced ventilation of the deeper parts of the basin. The formation of the DCM was in turn related to the shoaling of the pycnocline due to a reduced salinity of the Mediterranean Intermediate Water (MIW).

A refinement of the model was later provided by Castradori (1993) who, because of the detection of the deep-water calcareous nannofossil species *Florisphaera profunda*, suggested that Quaternary sapropel deposition was triggered by increased primary productivity, either confined to a DCM or extended to a thicker layer of the photic zone.

Sancetta (1994) proposed a further mechanism able to form sapropels: fluvial waters from the continents enhance productivity by supplying a high concentration of dissolved nutrients, and by stratify-

ing the surface waters because of low salinity. This results in a bloom dominated by diatoms. The bloom occurs too rapidly for most zooplankton to respond, and thus is not limited by grazing pressure. Mats, originated during repeated events, rapidly sink to the seafloor, and are preserved even in the presence of oxygenated bottom waters because of the high tensile strength and impenetrability of the diatom meshwork, thus leading to the formation of packets of laminae and the distinctive sapropel strata. Thus, according to Sancetta (1994), surface density stratification leads to sapropel formation via high primary production and rapid carbon flux; this model can be applied at least to sapropels showing laminated diatomaceous sediment.

Miocene sapropels have received much less attention than those younger, but Nijenhuis et al. (1996) and Schenau et al. (1998) by examining the paleonto-

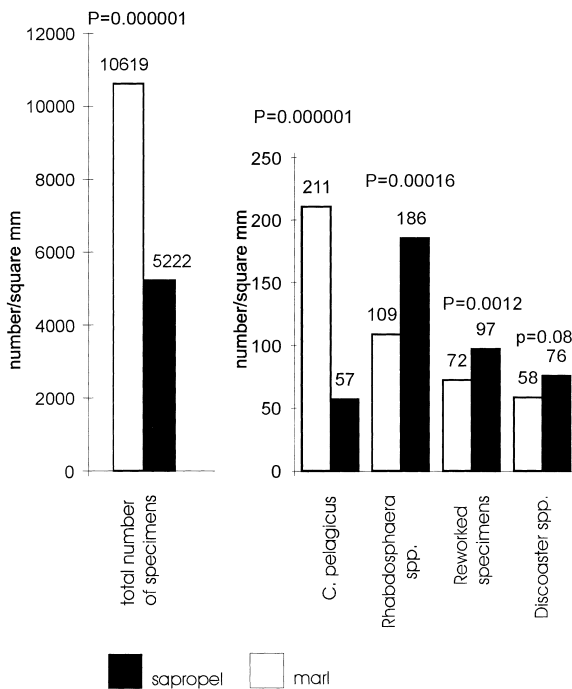


Fig. 8. Mean values of the total number of specimens, *Rhabdosphaera* spp., *Discoaster* spp., *C. pelagicus* and reworked specimens in sapropels and marls. *T*-test results (*P*) are shown at the top of bars. The significance threshold is 0.05.

logical (foraminifers) and geochemical (Ba, Co, and V content) data point out strong similarities with the younger sapropels. Furthermore the finding of *F. profunda* in Pliocene sapropels showing the same patterns as in the Quaternary ones (*F. profunda* increases in abundance in basal Zanclean sapropel sediments

at ODP site 969b, Castradori, 1997) appears to corroborate the hypothesis that a single mechanism has driven sapropel deposition during the last 10 Myr.

In our study we have observed some peculiar features in the calcareous nannofossil assemblage in sapropels, which can be synthesized as follows (Fig. 5):

- (1) increase of genus *Discoaster*;
- (2) among *Discoaster*, increase of *D. pentaradiatus*;
- (3) among *Discoaster* decrease of *D. intercalaris*;
- (4) decrease of *C. pelagicus*;
- (5) decrease of the total number of coccoliths (carbonate productivity);
- (6) increase of *Rhabdosphaera* spp.;
- (7) increase of reworked specimens.

To check the statistical validity of these inferences, based on the visual correlation between positive or negative fluctuations and sapropels, we performed statistical *T*-test analyses whose results are shown in Fig. 8 and Table 2. The mean abundances of *C. pelagicus*, *Rhabdosphaera* spp. and of the reworked specimens were significantly different ( $P < 0.002$ ), despite relatively wide standard deviations, in comparing sapropels with marls. For the discoasterids the difference between sapropels and marls did not reach a statistical significance ( $P = 0.08$ ).

## 6. Discussion

According to Haq (1980) and Lohmann and Carlson (1981) discoasterids are widely distributed in

Table 2  
Descriptive statistics of selected species abundances in marls and sapropels

	Total number of specimens	<i>C. pelagicus</i>	<i>Rhabdosphaera</i> spp.	<i>Discoaster</i> spp.	Reworked specimens
<i>Marl (111)</i>					
Mean	10619	211	109	58	72
Standard deviation	5162	151	88	43	33
Standard error of mean	490	14	8	4	3
Confidence interval (95%)	960	28	16	8	6
<i>Sapropel (27)</i>					
Mean	5222	57	186	76	97
Standard deviation	2983	30	104	60	45
Standard error of mean	574	6	20	11	9
Confidence interval (95%)	1125	11	39	23	17

the open ocean at low latitudes in tropical and subtropical areas. In the present study, although the difference in discoaster abundances between sapropels and marls do not reach full statistical significance ( $P = 0.08$ ) (Fig. 8), an interesting trend has been found (Fig. 5). In particular it is remarkable that *D. pentaradiatus* and *D. intercalaris*, the former related to warm conditions (Bukry, 1974) while the latter is interpreted as a cold morphotype of *D. variabilis* (Bukry, 1971), show a complementary behavior: an increase in the abundance of *D. pentaradiatus* corresponds to a decrease of *D. intercalaris*.

Another important paleoclimatic marker is *C. pelagicus* which has been related to low temperature conditions (Raffi and Rio, 1981). Our statistical analyses highlights significantly lower abundances of *C. pelagicus* in sapropels (Fig. 8). In addition, in the section examined, negative fluctuations of *C. pelagicus* abundance, are associated in sapropels with increased abundance of discoasterids and *D. pentaradiatus*. These considerations suggest an alternation of cold/warm conditions related to sapropel deposition. Sapropels in particular show an apparently warm nannofossil assemblage, an observation in agreement with Calieri (1996) who estimated in the Faneromeni section an increase of the SST corresponding to these peculiar layers.

Another characteristic observed in sapropels is the decrease in abundance of the total number of coccoliths. It is known that coccolithophorids generally bloom in conditions of oligotrophy (Ziveri et al., 1995a,b), and negatively correlate to diatom fluxes. Diatoms are in fact known to have a competitive advantage when nutrient levels and supply rates are high (Ziveri et al., 1995b; Sancetta, 1996). Schrader and Matherne (1981) and more recently Kemp et al. (1997) discovered the occurrence in the late Quaternary sapropel S-5 of laminated sediments rich in diatoms. According to this finding, the proposed mechanism (Sancetta, 1994) in which a bloom in siliceous plankton related to increased supply of nutrients produces sapropel sediments, appears plausible. Since siliceous remains are not always preserved because of their low resistance to dissolution [i.e. high silica unsaturation in the first 1000 m of the water column (Hurd and Theyer, 1975; Kennett, 1982)] Negri et al. (1998) proposed that the negative fluctuation in the total amount of nannofossils

in late Quaternary sapropels could imply a decrease in productivity of this group as well as the occurrence of a diatom bloom even when fossils of the diatoms are not preserved. However, currently no positive evidence on the existence of diatom blooms in these sapropel intervals are available and thus this interpretation remains speculative.

As for the positive fluctuations of *Rhabdosphaera* spp. in sapropels, this feature has been already observed by Castradori (1993) and Negri et al. (1998) in the late Quaternary sapropels. Roth and Coulbourn (1982) considered *Rhabdosphaera* spp. opportunistic species able to survive also in low nutrient conditions. Haidar and Thierstein (1997) confirm this hypothesis and relate these forms to low nutrient and high temperature and light intensity. In addition Ziveri et al. (1995a) observed *Rhabdosphaera* spp. in modern assemblages over a wide range of SSTs (14–20°C). In the late Quaternary sapropels the increase of *Rhabdosphaera* spp. and *F. profunda* are positively correlated (Castradori, 1992; Negri et al., 1998). The significance of the increased abundance of *F. profunda* in sapropels was thoroughly explained by Castradori (1993), who related this feature to enhanced paleoproductivity, either restricted to a Deep Chlorophyll Maximum, or extended to a thicker layer of the euphotic zone during the deposition of such sediments. At first, this appears to suggest that an increase in *Rhabdosphaera* spp. can be related to the presence of a DCM, even when *F. profunda* is lacking (e.g. in Miocene sediments). However, we must keep in mind that the present ecological requirements of *F. profunda* are not unambiguously known. In fact, Ahagon et al. (1993) recognized a close relationship between the increase of *F. profunda* abundance and increased water-transparency. In contrast, in modern coccolithophore assemblages *F. profunda* increases during the cold season (January–February) when coccolithophorids bloom (Ziveri et al., 1995a), thus it appears to prefer nutrient depleted water characterized also by low light intensity and low temperature. Therefore, it is not clear if *F. profunda* can be related to the presence of a DCM and consequently if the *Rhabdosphaera* spp. increase in sapropels is related either to a DCM, or more likely to its opportunistic behavior, that makes this taxon able to flourish at the end of the siliceous plankton bloom, when the water becomes impoverished in nutrients. In any case it is

evident that the *Rhabdosphaera* spp. increase represents a consistent feature characterizing these layers during the last 10 Myr.

Finally, the regular increase of reworked specimens in sapropels is a very unusual feature already observed by Negri et al. (1998) in late Quaternary sapropels. Reworking often affects calcareous nanofossil thanatocoenoses. In biostratigraphy it is a problem whose effects have been reduced after the introduction of quantitative methodologies (Rio et al., 1990). Furthermore, by means of quantitative analyses we can now evaluate the fluctuations in abundance of reworked specimens, which in some cases are correlated with specific sediment types (e.g. turbidites). In this study peaks in the abundance of reworked specimens correlate to sapropel layers (Fig. 5). It is known that rivers convey to their mouths large amounts of suspended sediment that is generally deposited in the fan, but the fine detritus can be transported well beyond the fan. As suggested by Negri et al. (1998), during sapropel deposition the increased fluvial runoff and discharge probably enhanced this phenomenon. Thus, the observed peaks in the abundance of reworked specimens may be a strong evidence of increased river discharge from the lands surrounding the basin (i.e. Alps) and consequently of the formation of low salinity, nutrient rich surface water.

## 7. Conclusions

The detailed calcareous nanofossil quantitative and semiquantitative analysis performed on 138 samples from the M. del Casino section allow us to recognize the most important bioevents for the Tortonian–Messinian interval. Among the *Amaurolithus* genus the first occurrences of *A. primus*, *A. cf. amplificus* and *A. delicatus* have been recognized. Further bioevents, such as the acme beginning and the acme end of small reticulofenestrids (*Reticulofenestra minuta* and *Dictyococcites productus*), and the FO, FCO and LO of *R. rotaria* appear to be useful for the improvement of the biostratigraphic resolution of the T/M boundary interval, at least for the Mediterranean area.

Quantitative analyses of calcareous nanofossils show distinctive fluctuations in the calcareous nan-

nofossil assemblage characterizing sapropel layers. A decrease in the total abundance of coccoliths and *C. pelagicus*, and an increase in the abundance of genus *Rhabdosphaera*, *Discoaster*, and reworked specimens correspond to sapropels.

The most likely interpretation suggests that during periods characterized by warmer temperatures (indicated by the increase in abundance of the *Discoaster* group and the concurrent decrease of *C. pelagicus*), increased total productivity (associated with a decrease in the number of coccoliths) and the presence of reduced salinity surface waters (suggested by an increase of reworked coccoliths) could be the cause of the deposition of sapropels. In any case, strong paleontological similarities with younger sapropels are evident, thus suggesting that knowledge of the ecological requirements of species in modern assemblages is a key point to clearly understand the mechanism of sapropel deposition. A unique mechanism appears to drive the deposition of sapropels during the last 10 Myr.

## Acknowledgements

Giuliana Villa is warmly thanked for the helpful discussion and advises to the first draft. The critical reviews by Elisabetta Erba and Eliana Fornaciari improved the original manuscript.

## Appendix A. Taxonomic appendix

All species are pictured in Plankton Stratigraphy edited by Bolli et al. (1985) and in Theodoridis (1984).

- Amaurolithus amplificus* (Bukry and Percival, 1971) Gardtner and Bukry, 1975
- Amaurolithus delicatus* Gardtner and Bukry, 1975
- Amaurolithus primus* (Bukry and Percival, 1971) Gardtner and Bukry, 1975
- Calcidiscus leptoporus* (Murray and Blackman, 1898) Loeblich and Tappan, 1978
- Coccolithus pelagicus* (Wallich, 1877) Schiller, 1930
- Discoaster asymmetricus* Gartner, 1969
- Discoaster brouweri* Tan, 1927, emend. Bramlette and Riedel, 1954
- Discoaster challengerii* Bramlette and Riedel, 1954
- Discoaster icarus* Stradner, 1973
- Discoaster loeblichii* Bukry, 1971
- Discoaster intercalaris* Bukry, 1971

*Discoaster pentaradiatus* Tan, 1927, emend. Bramlette and Riedel, 1954

*Discoaster tamalis* Kamptner, 1967

*Discoaster variabilis* Martini and Bramlette, 1963

*Dictyococcites productus* (Kamptner, 1973) Backman, 1980

*Florisphaera profunda* Okada and Honjo, 1973

*Geminiolithella rotula* (Kamptner, 1956) Backman, 1980

*Helicosphaera carteri* (Wallich, 1877) Kamptner, 1954

*Helicosphaera intermedia* Martini, 1965

*Helicosphaera orientalis* Black, 1971

*Helicosphaera sellii* Bukry and Bramlette, 1969

*Helicosphaera stalis* Theodoridis, 1984

*Helicosphaera walbersdorfensis* Muller, 1974

*Reticulofenestra rotaria* Theodoridis, 1984

*Reticulofenestra minuta* Roth, 1970

*Rhabdosphaera claviger* Murray and Blackman, 1898

*Rhabdosphaera stylifer* Lohmann, 1902

*Syracosphaera pulchra* Lohmann, 1902

Supraspecific categories:

*Braarudosphaera* spp. Deflandre, 1947

*Pontosphaera* spp. Lohmann, 1902

*Rhabdosphaera* spp. Haeckel, 1894

*Reticulofenestra* spp. Hay, Mohler and Wade, 1966

*Scyphosphaera* spp. Lohmann, 1902

*Syracosphaera* spp. Lohmann, 1902

*Thoracosphaera* spp. Kamptner, 1927

## References

- Ahagon, N., Tanaka, Y., Ujiie, H., 1993. *Florisphaera profunda*, a possible nannoplankton indicator of late Quaternary changes in seawater turbidity at the northwestern margin of the Pacific. *Mar. Micropaleontol.* 22, 255–273.
- Backman, J., 1978. Late Miocene–Early Pliocene nannofossil biochronology and biogeography in the Vera Basin, SE Spain. *Stockholm Contrib. Geol.* 32 (2), 93–114.
- Bolli, H.M., Saunders, J.B., Perch Nielsen, K., 1985. *Plankton Stratigraphy*, Vol. 1. Cambridge Univ. Press, Cambridge, 599 pp.
- Bukry, D., 1971. Cenozoic calcareous nannofossils from the Pacific ocean. *Trans. San Diego Soc. Nat. Hist.* 16, 303–327.
- Bukry, D., 1974. Phytoplankton stratigraphy, offshore East Africa, Deep Sea Drilling Project Leg 25. *Init. Rep. DSDP* 25, 635–646.
- Calieri, R., 1992. Stratigrafia analisi paleoclimatica e radiometria del Tortoniano superiore–Messiniano pre-evaporitico nell'Appennino Romagnolo (M. del Casino–M.te Tondo). Thesis, Univ. Bologna, 79 pp. (unpubl.).
- Calieri, R., 1996. Planktonic foraminiferal biostratigraphy and cyclostratigraphy of the Tortonian Messinian boundary: preliminary results from the Faneromeni section (Crete). *Paleoelagias* 6, 329–339.
- Calieri, R., 1997. Biostratigrafia e cicli paleoclimatologici del Messiniano inferiore (confronto tra i sedimenti del versante adriatico e quelli del mediterraneo orientale). Ph.D. Thesis, Roma and Firenze National Library, 107 pp.
- Calvert, S.E., 1983. Geochemistry of Pleistocene sapropel and associated sediments from the Eastern Mediterranean. *Oceanol. Acta* 6, 255–267.
- Cande, S.C., Kent, D.V., 1992. A new geomagnetic polarity time scale for the Late Cretaceous and Cenozoic. *J. Geophys. Res.* 97, 13917–13951.
- Cande, S.C., Kent, D.V., 1995. Revised calibration of the geomagnetic polarity time scale for the Late Cretaceous and Cenozoic. *J. Geophys. Res.* 100, 6093–6095.
- Castradori, D., 1992. I nannofossili calcarei come strumento per lo studio biostratigrafico e paleoceanografico del Quaternario nel Mediterraneo Orientale. Ph.D. Thesis, Roma and Firenze National Library, 216 pp.
- Castradori, D., 1993. Calcareous nannofossils and the origin of eastern Mediterranean sapropels. *Paleoceanography* 8, 459–471.
- Castradori, D., 1997. Calcareous nannofossil distribution patterns in the basal Zanclean of the deep Mediterranean sea. *Int. Conf. on Neogene Paleocyanography*, Erice, Italy, 28–30 September 1997, pp. 15–16 (abstract).
- Cita, M.B., Vergnaud-Grazzini, C., Robert, C., Chamley, H., Ciaranfi, N., D'Onofrio, S., 1977. Paleoclimatic record of a long deep sea core from the eastern Mediterranean. *Quat. Res.* 8, 205–235.
- Colalongo, M.L., Di Grande, A., D'Onofrio, S., Giannelli, L., Iaccarino, S., Mazzei, R., Poppi Brigatti, M.F., Romeo, M., Rossi, A., Salvatorini, G., 1979. A proposal for the Tortonian/Messinian boundary. *Ann. Geol. Pays Hell. Tome Hors Ser. 1*, 285–294.
- De Kaenel, E., Villa, G., 1996. Oligocene–Miocene calcareous nannofossil biostratigraphy and paleoecology from the Iberia abyssal plain. *Proc. ODP Sci. Results* 149, 79–145.
- Ferretti, S., Terzi, C., 1995. Late Miocene isotope stratigraphy and astronomical calibration of the Monte del Casino section (northern Apennines, Italy). *G. Geol.* 57 (12), 99–112.
- Flores, J.A., Sierro, F.J., 1987. Calcareous plankton in the Tortonian/Messinian transition series of the Northwestern edge of the Guadalquivir basin. *Abh. Geol. Bundesanst.* 39, 67–84.
- Flores, J.A., Sierro, F.J., Glaçon, G., 1992. Calcareous plankton analysis in the pre-evaporitic sediments of the ODP Site 654 (Tyrrhenian Sea, Western Mediterranean). *Micropaleontology* 38 (3), 279–288.
- Gartner, S., 1992. Miocene nannofossil chronology in the North Atlantic, DSDP Site 608. *Mar. Micropaleontol.* 18, 307–331.
- Haidar, A.T., Thierstein, H.R., 1997. Calcareous Phytoplankton Dynamics at Bermuda (N. Atlantic). *EUG 9 Abstr. Suppl. 1*. Terra Nova 9, 602.
- Haq, B.U., 1980. Biogeographic history of Miocene calcareous nannoplankton and paleoceanography of the Atlantic Ocean. *Micropaleontology* 26 (4), 414–443.
- Hilgen, F.J., Krijgsman, W., Langereis, C.G., Lourens, L.J., Santarelli, A., Zachariasse, W.J., 1995. Extending the astronomical (polarity) time scale into the Miocene. *Earth Planet. Sci. Lett.* 136, 495–510.

- Hodell, D.A., Benson, R.H., Kent, D.V., Boersma, A., Rakic-El Bied, K., 1994. Magnetostratigraphic, biostratigraphic, and stable isotope stratigraphy of an Upper Miocene drill core from the salé Briqueterie (northwestern Morocco): A high-resolution chronology for the Messinian stage. *Paleoceanography* 9 (6), 835–855.
- Hurd, D.C., Theyer, F., 1975. Changes in the Physical and chemical properties of biogenic silica from the central equatorial Pacific. *Adv. Chem. Ser.* 147, 211–230.
- Kemp, A.E.S., Pearce, R.B., Rance, J., Cramp, A., 1997. A laminated diatom ooze 'S5' from the Eastern Mediterranean: implications for sapropel origins. *EUG 9 Abstr. Suppl. 1. Terra Nova* 9, 402.
- Kennett, J.P., 1982. *Marine Geology*. Prentice-Hall, Englewood Cliffs, NJ, 813 pp.
- Krijgsman, W., Hilgen, F.J., Langereis, C.G., Zachariasse, W.J., 1994. The age of the Tortonian/Messinian Boundary. *Earth Planet. Sci. Lett.* 121, 533–547.
- Krijgsman, W., Hilgen, F.J., Langereis, C.G., Santarelli, A., Zachariasse, W.J., 1995. Late Miocene magnetostratigraphy, biostratigraphy and cyclostratigraphy from the Mediterranean. *Earth Planet. Sci. Lett.* 136, 475–494.
- Krijgsman, W., Hilgen, F.J., Negri, A., Wijbrans, J.R., Zachariasse, W.J., 1997. The Monte del Casino section (Northern Apennines, Italy): a potential Tortonian/Messinian boundary stratotype? *Palaeogeogr., Palaeoclimatol., Palaeoecol.* 133, 27–47.
- Lohmann, G.P., Carlson, J.J., 1981. Oceanographic significance of Pacific Late Miocene calcareous nannoplankton. *Mar. Micropaleontol.* 6, 553–579.
- Martini, E., 1971. Standard Tertiary and Quaternary calcareous nannoplankton zonation. *Proc. II Planktonic Conf., Roma* 1970, 2, 739–785.
- Mazzei, R., Raffi, I., Rio, D., Hamilton, N., Cita, M.B., 1979. Calibration of late Neogene calcareous plankton datum planes with the paleomagnetic record of Site 397 and correlation with Moroccan and Mediterranean sections. *Init. Rep. DSDP* 47 (1).
- Negri, A., Vigliotti, L., 1997. Calcareous nannofossil biostratigraphy and paleomagnetism of the Monte Tondo and Monte del Casino sections (Romagna Apennine, Italy). In: Montanari, A., Odin, G.S., Coccioni, R. (Eds.), *Miocene Stratigraphy: An Integrated Approach*. *Dev. Paleontol. Stratigr.* 15, 477–493.
- Negri, A., Capotondi, L., Keller, J., 1998. Calcareous nannofossils and planktic foraminifers distribution patterns in Late Quaternary–Holocene sapropels of the Ionian Sea. *Mar. Geol.* (in press).
- Nijenhuis, I.A., Schenau, S.J., Van der Weijden, C.H., Hilgen, F.J., Lourens, L.J., Zachariasse, W.J., 1996. On the origin of upper Miocene sapropelites: A case study from the Faneromeni section, Crete (Greece). *Paleoceanography* 11, 633–645.
- Okada, H., Bukry, D., 1980. supplementary modification and introduction of code numbers to the low-latitude coccolith biostratigraphic zonation (Bukry, 1973; 1975). *Mar. Micropaleontol.* 5, 321–325.
- Olausson, E., 1961. Studies of deep-sea cores. *Rep. Swed. Deep Sea Exped. 1947–1948* 8, 353–391.
- Parisi, E., 1987. Carbon and oxygen isotope composition of *Globigerinoides ruber* in two deep sea cores from the Levantine Basin (Eastern Mediterranean). *Mar. Geol.* 75, 201–219.
- Pedersen, T.F., Calvert, S.E., 1990. Anoxia vs. productivity: what controls the formation of organic-carbon-rich sediments and sedimentary rocks? *AAPG Bull.* 74, 454–466.
- Raffi, I., Flores, F., 1995. Pleistocene through Miocene calcareous nannofossils from eastern equatorial Pacific Ocean (Leg 138). *Proc. ODP Sci. Results* 138, 233–286.
- Raffi, I., Rio, D., 1981. *Coccolithus pelagicus* (Wallich): a paleotemperature indicator in the late Pliocene Mediterranean deep sea record. In: Wezel, F.C. (Ed.), *Sedimentary Basins of Mediterranean Margins*. pp. 187–190.
- Raffi, I., Rio, D., D'Atri, A., Fornaciari, E., Rocchetti, S., 1995. Quantitative distribution patterns and biomagnetostratigraphy of middle to late Miocene calcareous nannofossils from Equatorial Indian and Pacific Oceans (Legs 115, 130, 138). *Proc. ODP Sci. Results* 138, 479–502.
- Rakic El Bied, K., Benson, R.H., 1996. La stratigraphie a Haute Resolution: Theorie et application au Neogen superieur du Maroc. *Notes Mem. Serv. Geol. Maroc* 383, 5–50.
- Rio, D., Raffi, I., Villa, G., 1990. Pliocene–Pleistocene calcareous nannofossil distribution patterns in the Western Mediterranean. *Proc. ODP Sci. Results* 107, 513–533.
- Rohling, E.J., Gieskes, W.W.C., 1989. Late Quaternary changes in Mediterranean Intermediate Water density and formation rate. *Paleoceanography* 4, 531–545.
- Rossignol Strick, M., 1983. African monsoon an immediate climate response to orbital insolation. *Nature* 304, 46–49.
- Rossignol Strick, M., 1985. Mediterranean Quaternary sapropels, an immediate response of the African monsoon to variations of insolation. *Palaeogeogr., Palaeoclimatol., Palaeoecol.* 49, 237–263.
- Roth, P.H., Coulbourn, W.T., 1982. Floral and solution patterns of coccoliths in surface sediments of the North Pacific. *Mar. Micropaleontol.* 7, 1–52.
- Ryan, W.B.F., 1972. Stratigraphy of Late Quaternary Sediments in the Eastern Mediterranean. In: Stanley, D.J. (Ed.), *The Mediterranean Sea*. Dowden, Hutchinson and Ross, Stroudsburg, PA, pp. 149–169.
- Sancetta, C., 1994. Mediterranean sapropels: Seasonal stratification yields high production and carbon flux. *Paleoceanography* 9, 195–196.
- Sancetta, C., 1996. Laminated diatomaceous sediments: controls on formations and strategies for analysis. In: Kemp, A.E.S. (Ed.), *Paleoclimatology and Palaeoceanography from Laminated Sediments*. *Geol. Soc. Spec. Publ.* 116, 17–23.
- Schenau, S.J., Antonarakou, A., Hilgen, F.J., Lourens, L.J., Nijenhuis, I.A., Van der Weijden, C.H., Zachariasse, W.J., 1998. Organic-rich layers in the Metochia section (Gavdos, Greece): evidence for a single sapropel formation mechanism in the eastern Mediterranean during the last 10 Myr (in press).
- Schrader, H.J., Matherne, A., 1981. Sapropel formation in the eastern Mediterranean Sea: evidence from preserved opal assemblage. *Micropaleontology* 27, 191–203.

- Siero, F.J., Flores, J., Civis, J., Gonzalez Delgado, I.A., Frances, G., 1993. Late Miocene globorotaliid event-stratigraphy and biogeography in the NE-Atlantic and Mediterranean. *Mar. Micropaleontol.* 21, 143–168.
- Tazzi, M., 1996. Biostratigrafia a nannofossili calcarei del limite Tortoniano/Messiniano nel bacino di Taza–Guercif (Marocco) e nel site 978 (Mare di Alboran). Thesis, Univ. Parma (unpubl.).
- Theodoridis, S., 1984. Calcareous nannofossils biozonation of the Miocene and revision of the Helicoliths and *Discoaster*. *Utrecht Micropaleontol. Bull.* 32, 1–271.
- Thunell, R.C., 1979. Pliocene–Pleistocene paleotemperature and paleosalinity history of the Mediterranean Sea: Results from DSDP Sites 125 and 132. *Mar. Micropaleontol.* 4, 173–187.
- Thunell, R.C., Williams, D.F., Kennett, J.P., 1977. Late Quaternary paleoclimatology, stratigraphy and sapropel history in eastern Mediterranean deep-sea sediments. *Mar. Micropaleontol.* 2, 371–388.
- Vai, G.B., Villa, I.M., Colalongo, M.L., 1993. First direct radiometric dating of the Tortonian/Messinian boundary. *C. R. Acad. Sci. Paris Ser. II* 316, 1407–1414.
- Violanti, D., Grecchi, G., Castradori, D., 1991. Paleoenvironmental interpretation of core Ban 88-11 GC (Eastern Mediterranean, Pleistocene–Holocene) on the grounds of Foraminifera, Thecosomata and calcareous nannofossils. *Quaternario* 4, 13–39.
- Ziveri, P., Thunell, R.C., Rio, D., 1995a. Seasonal changes in coccolithophore densities in the Southern California Bight during 1991–1992. *Deep-Sea Res. I* 42, 1881–1903.
- Ziveri, P., Thunell, R.C., Rio, D., 1995b. Export production of coccolithophores in an upwelling region: Results from San Pedro Basin, Southern California Borderlands. *Mar. Micropaleontol.* 24, 335–358.